Supporting Information

Content

Experimental Section

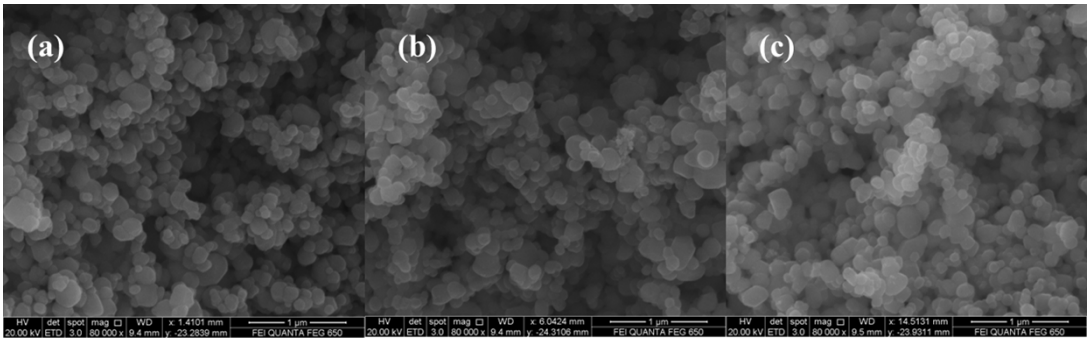

Figure S1. SEM image of (a) TiO_2 (b) Pd/TiO_2 and (c) Pt/TiO_2.

Summary Report

Surface Area

Single point surface area at P/Po = 0.254951315:	11.0895 m²/g
BET Surface Area:	12.2337 m²/g
Langmuir Surface Area:	51.2332 m²/g
t-Plot Micropore Area:	1.0105 m²/g
t-Plot external surface area:	11.2232 m²/g
BJH Adsorption cumulative surface area of pores between 1.7000 nm and 300.0000 nm diameter:	12.8044 m²/g
BJH Desorption cumulative surface area of pores between 1.7000 nm and 300.0000 nm diameter:	12.1893 m²/g

Pore Volume

t-Plot micropore volume:	0.000138 cm³/g
BJH Adsorption cumulative volume of pores between 1.7000 nm and 300.0000 nm diameter:	0.047246 cm³/g
BJH Desorption cumulative volume of pores between 1.7000 nm and 300.0000 nm diameter:	0.046204 cm³/g

Pore Size

Adsorption average pore diameter (4V/A by BET):	15.2674 nm
Desorption average pore diameter (4V/A by BET):	5.8623 nm
BJH Adsorption average pore diameter (4V/A):	14.7593 nm
BJH Desorption average pore diameter (4V/A):	15.1620 nm

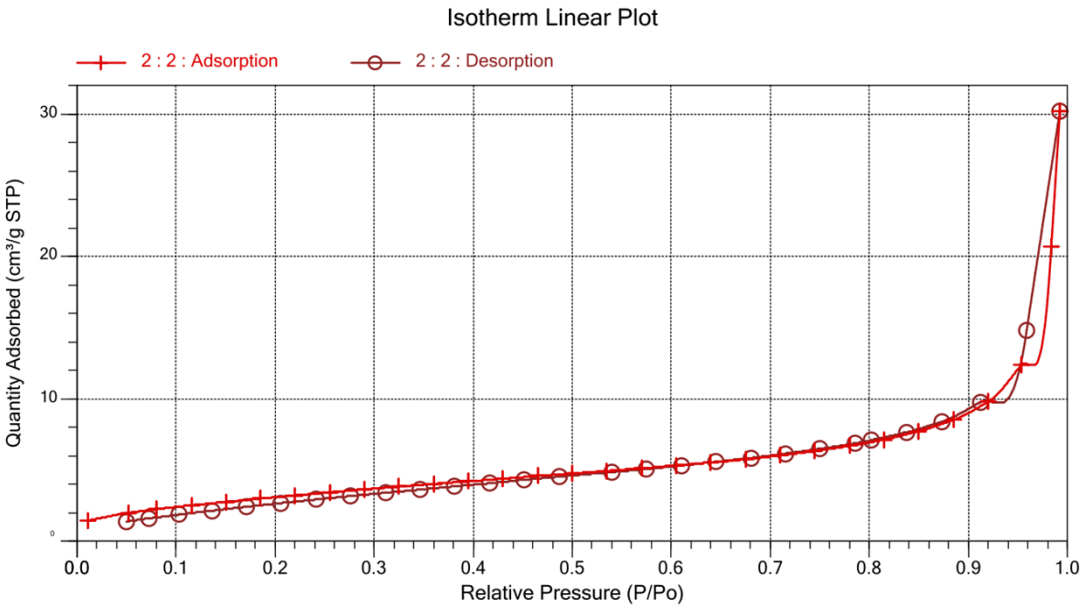

Figure S2. BET surface area and Nitrogen sorption isotherms at 77 K for Pd_1Pt_1/TiO_2

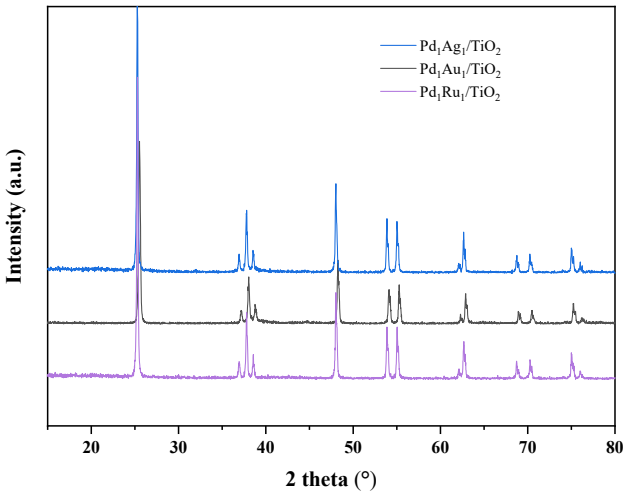

Figure S3. XRD diffraction patterns of other bimetallic photocatalysts.

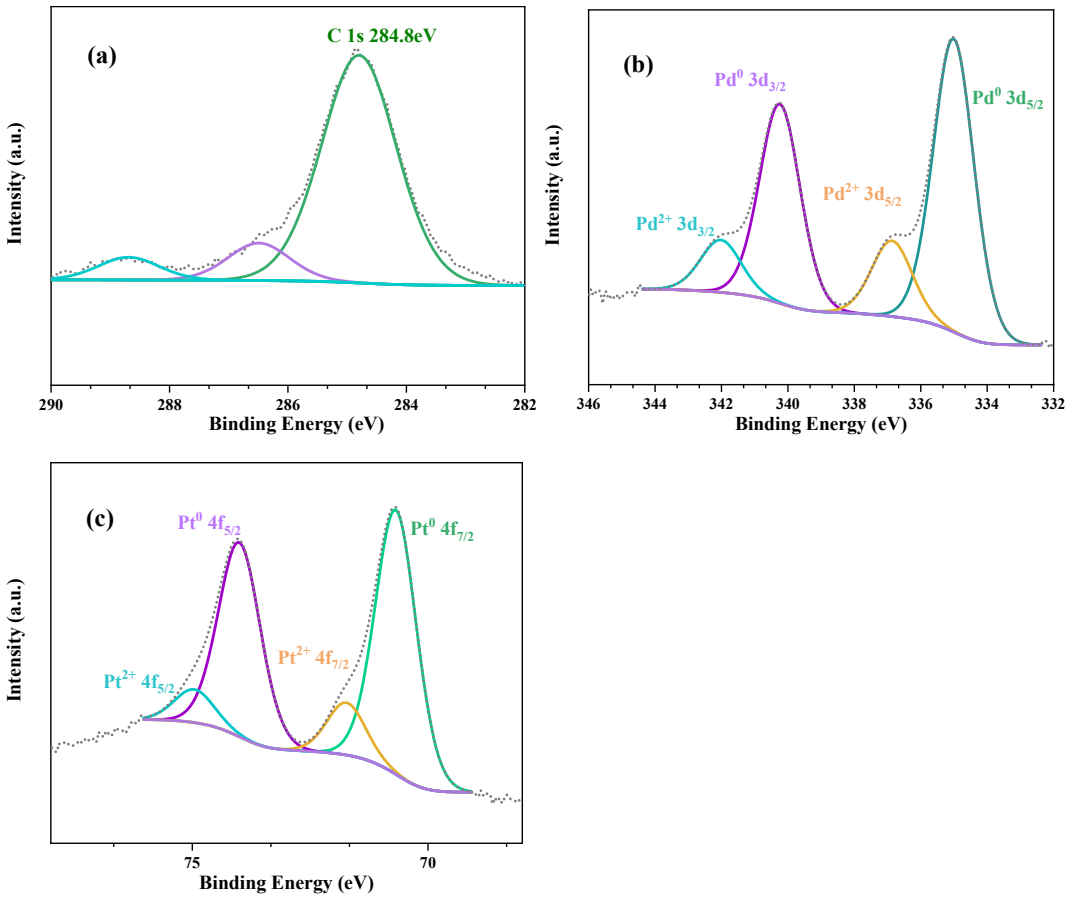

Figure S4. (a) core level spectra of C1s of Pd_1Pt_1/TiO_2. (b) XPS core level spectra of Pd $3d_{5/2}$ and $3d_{3/2}$ doublet region of Pd/TiO_2. (c) Pt $4f_{7/2}$ and $4f_{5/2}$ doublet region of Pt/TiO_2.

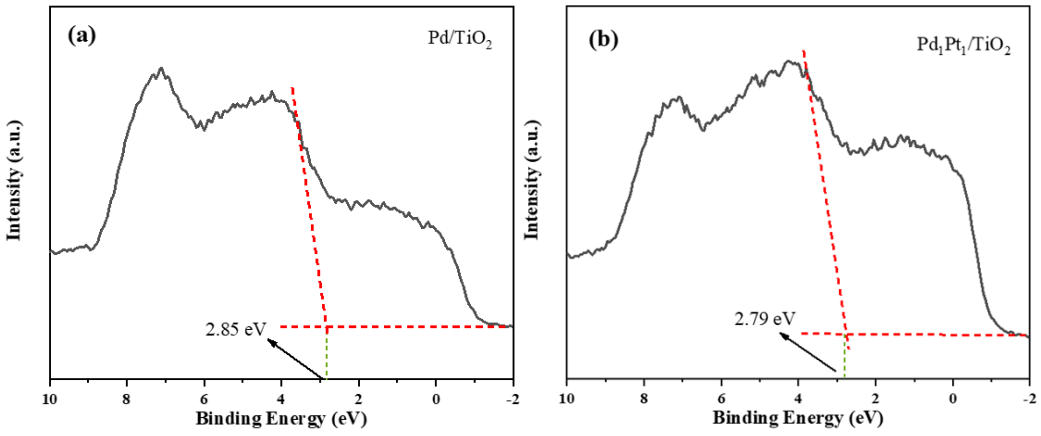

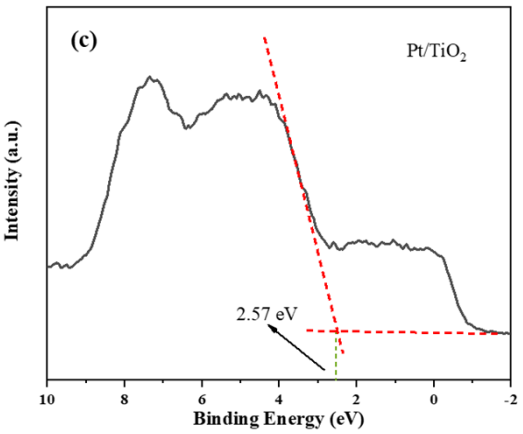

Figure S5. VB-XPS plots of (a) Pd/TiO_2 (b) Pd_1Pt_1/TiO_2 (c) Pt/TiO_2.

the E_{VB} of the corresponding standard hydrogen electrode ($E_{VB, NHE}$) can be calculated according to the following formula: $E_{VB, NHE} = \varphi + E_{VB, XPS} - 4.44$, where φ is the work function of the instrument (4.5 eV).[1]

Table S1. valence band edge potential (E_{VB}) and conductor band edge potential E_{CB} of various catalysts.

catalyst	E_{VB} (eV)	E_{CB} (eV)	Band gap (eV)
TiO_2	2.932	-0.312	3.244
Pd/TiO_2	2.906	-0.286	3.191
Pd_2Pt_1/TiO_2	2.905	-0.285	3.189
Pd_1Pt_1/TiO_2	2.891	-0.271	3.161
Pd_1Pt_2/TiO_2	2.891	-0.271	3.161
Pt/TiO_2	2.892	-0.271	3.163

Table S2. Benzaldehyde formed during photoreaction of benzyl alcohol with respective catalysts in the absence of amine.

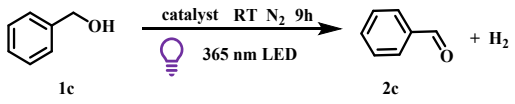

Entry	Catalyst	2c Yields. (%)

1	Pd/TiO_2	28
2	Pd_2Pt_1/TiO_2	43
3	Pd_1Pt_1/TiO_2	56
4	Pd_1Pt_2/TiO_2	65
5	Pt/TiO_2	71

Reaction conditions: benzyl alcohol (2.1 mmol), MeCN (5 ml), catalyst (10 mg), N_2, r.t., light irradiation (365 nm LED, 18 mW/cm^2), 9 h. The yields were obtained by HPLC.

Table S3. The yields of secondary amine 2d obtained during hydrogenation of imine 1d in methanol with respective catalysts.

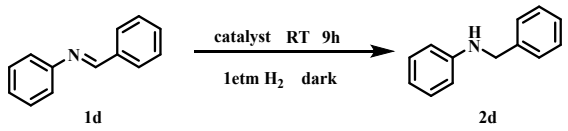

Entry	Catalyst	2d Yields. (%)
1	Pd/TiO_2	75
2	Pd_2Pt_1/TiO_2	86
3	Pd_1Pt_1/TiO_2	60
4	Pd_1Pt_2/TiO_2	43
5	Pt/TiO_2	10

Reaction conditions: N-Benzylideneaniline (2.1 mmol), methanol (5 ml), catalyst (10 mg), 1 atm H_2, r.t., 9 h. The yields were obtained by HPLC.

The details of product analysis and drawing of calibration curve

For aniline products, HPLC was used with calibration (C18 column, 30 °C, λ=254 nm, MeOH mobile phase, 1 mL min^{-1}), and the calibration curve was drawn by measuring the peak area of 0.025, 0.05, 0.1, 0.2, 0.5 mg/ml of standard sample. The calibration curve is as follows, and the HPLC yields were calculated as following formula:

$$HPLC\ yield = \frac{c \times 75 \times 5}{1.4 \times M}$$

Where the "c" represents for concentration obtained from calibration curve, "75" represent for dilution factor; "5" represent for volume of reaction solution; "M" represents for molecular weight of the product. Other products were analyzed by GC-FID using area normalization method.

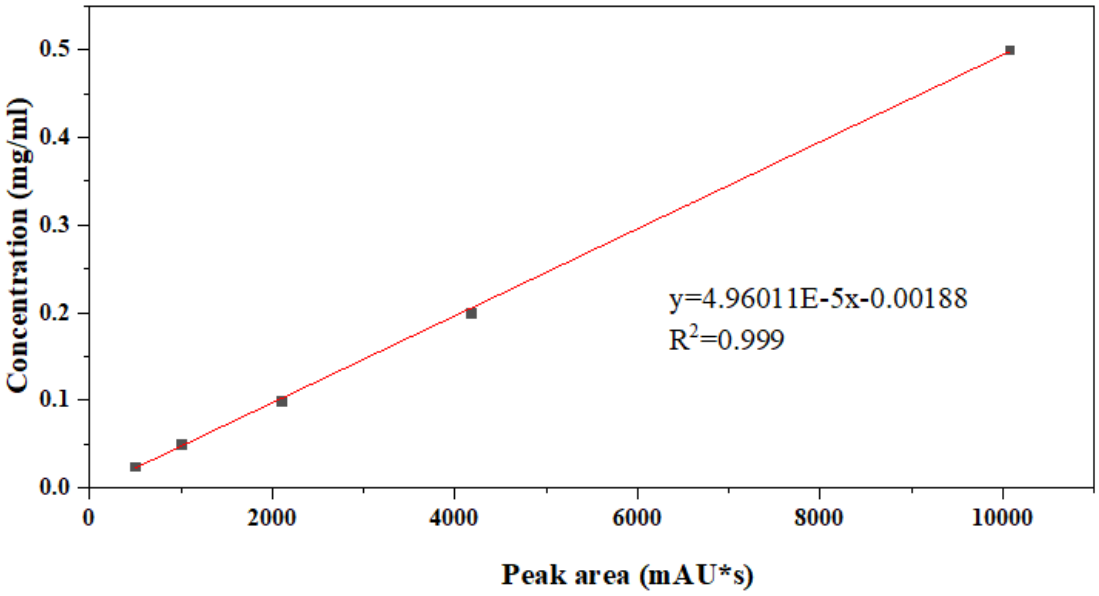

calibration curve of HPLC

MS spectra of all products

N,N-Dimethylaniline

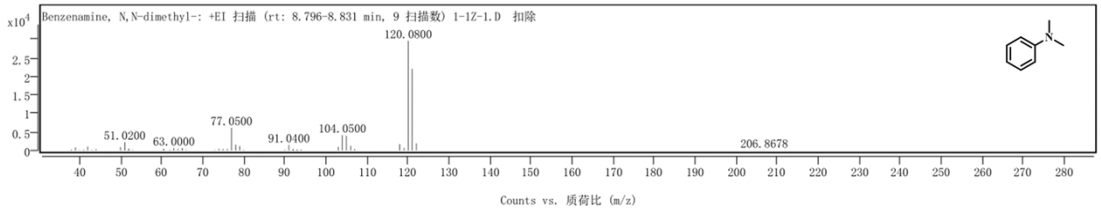

N-Benzyldiethylamine

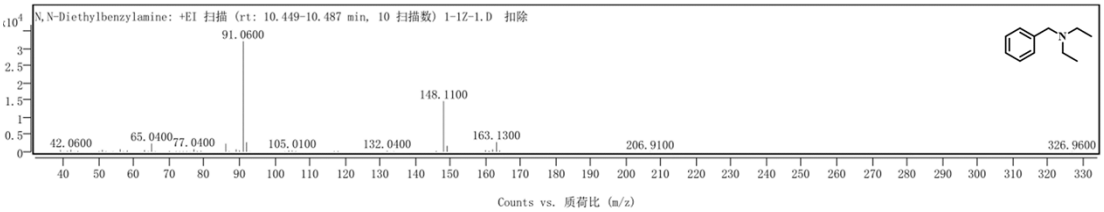

N-Benzylpropanamine

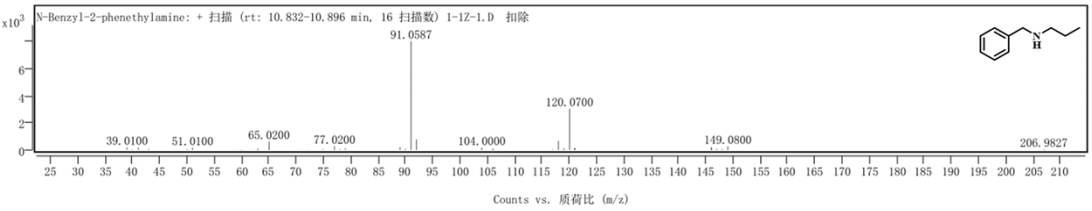

N-Butylaniline

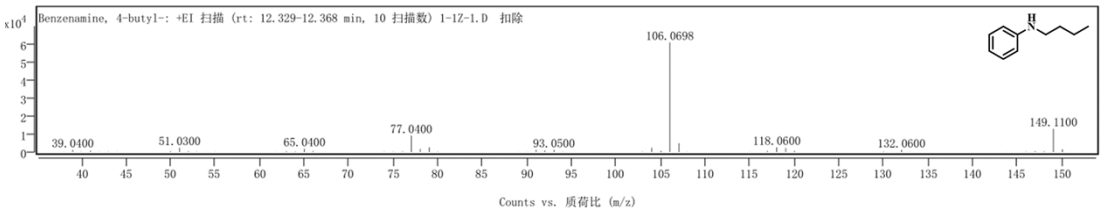

N-Benzylaniline

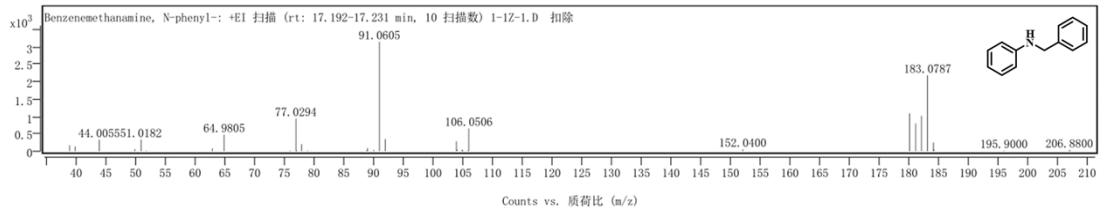

Dibenzylamine

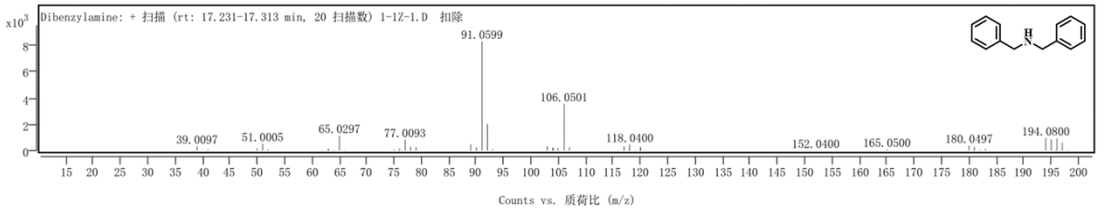

Diisopropylamine

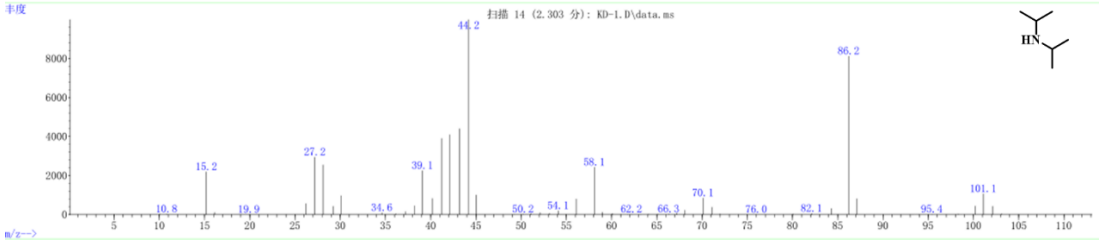

4-Methylmorpholine

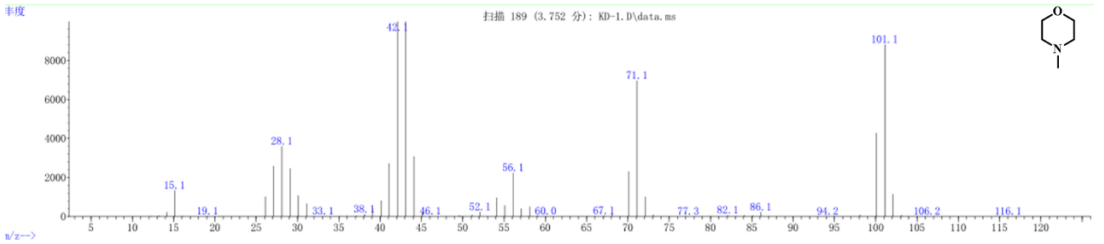

N,*N*,*N*′,*N*′-Tetramethylethylenediamine

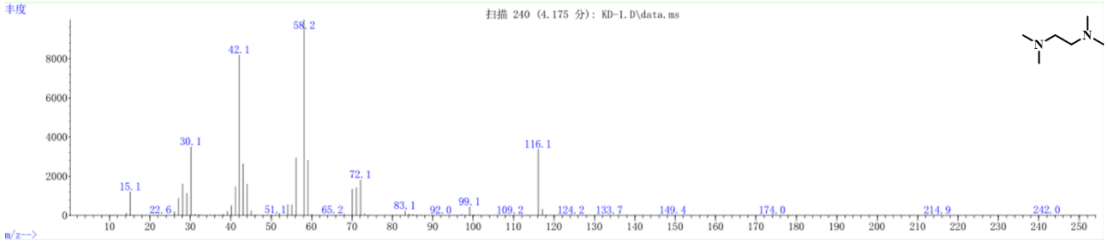

4-chloro-*N*,*N*-dimethylaniline

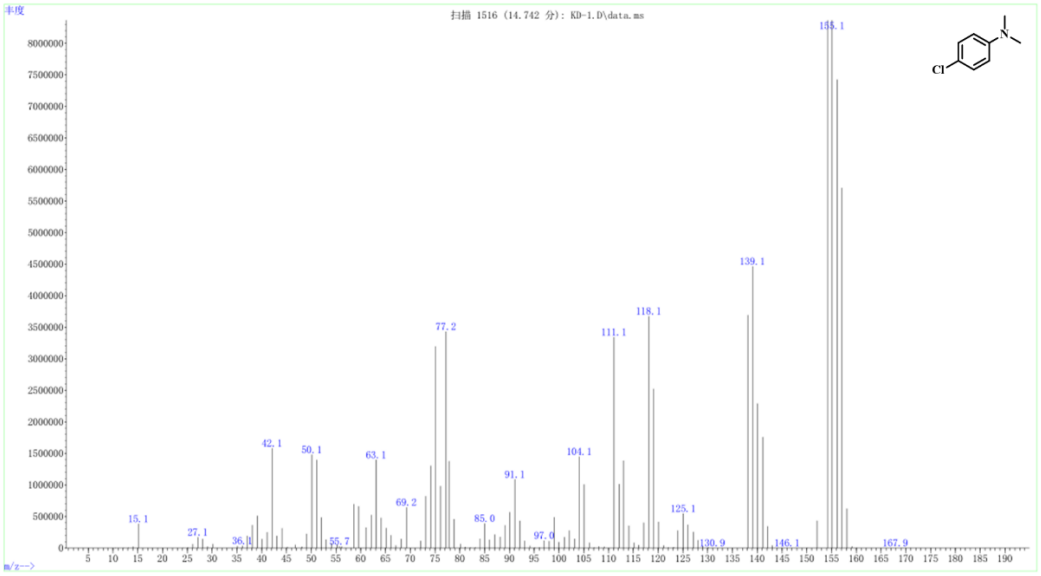

N,N-Diisopropylethylamine

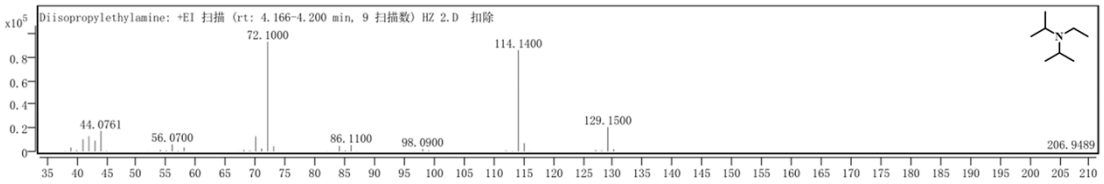

1-Ethylpiperidine

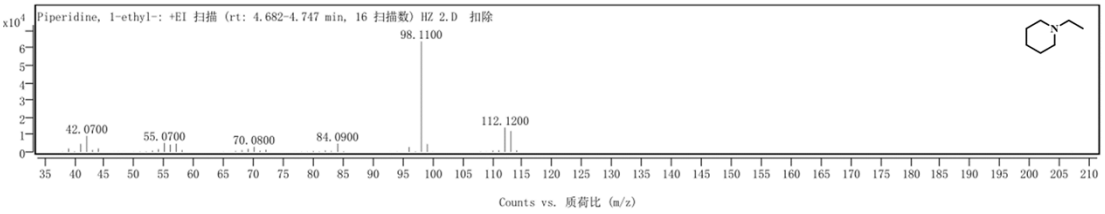

N,N-Dimethylcyclohexanamine

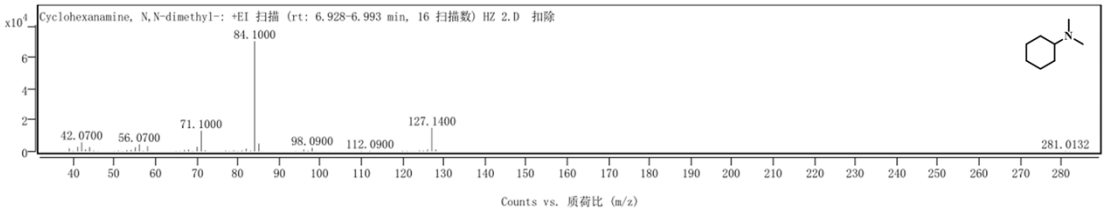

1,2,2,6,6-Pentamethylenepiperidine

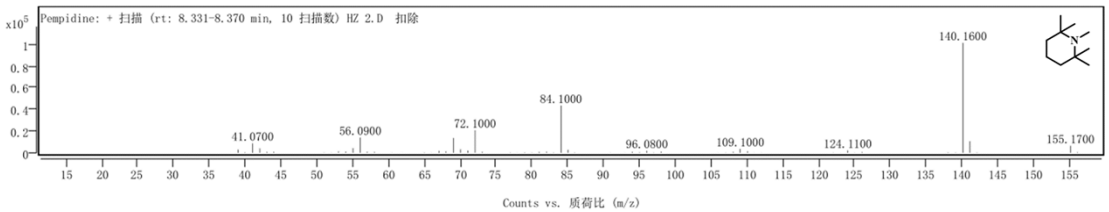

N,N-Diethylaniline

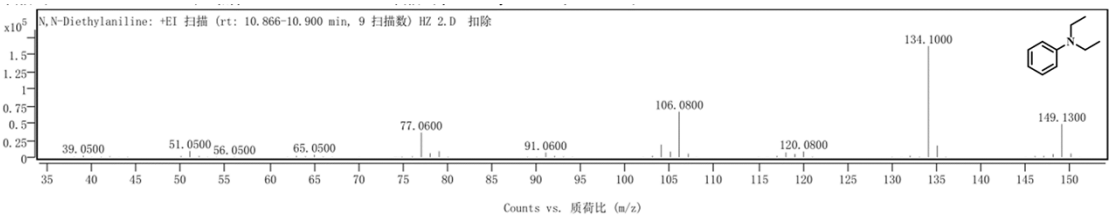

Benzyldiisopropylamine

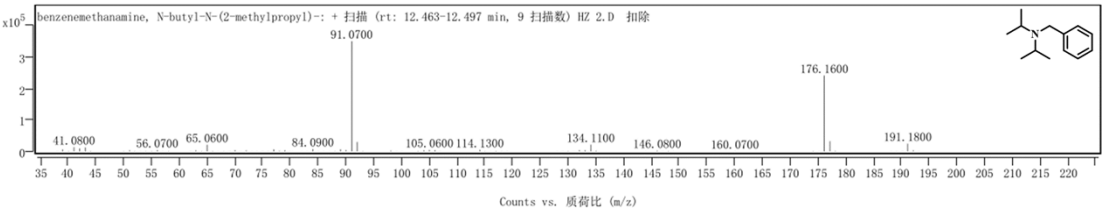

***N*-isopropylethylamine**

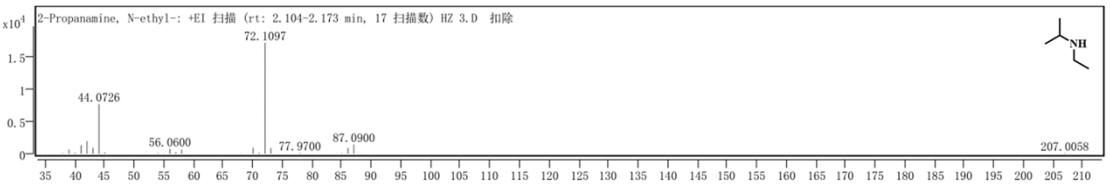

***N,N*-Diisopropylmethylamine**

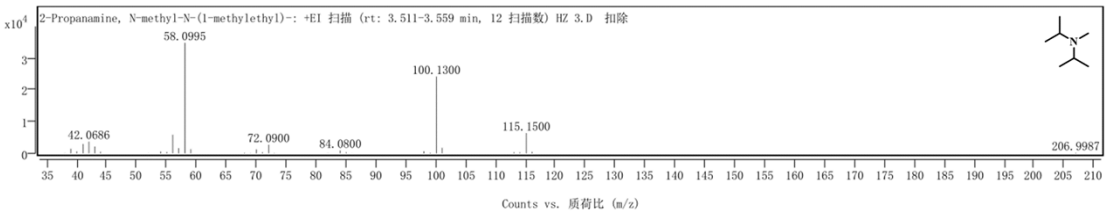

***N,N*-Dimethylcyclohexanamine**

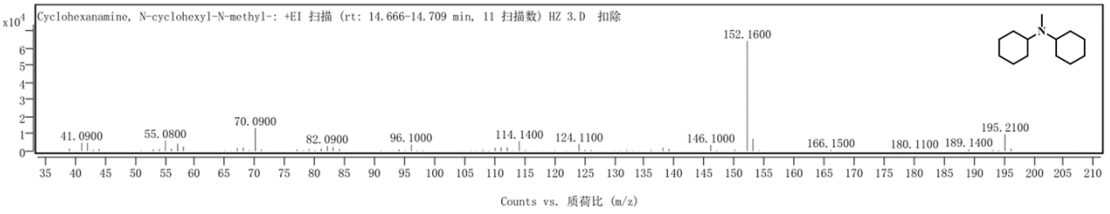

***N*-Methyldiphenylamine**

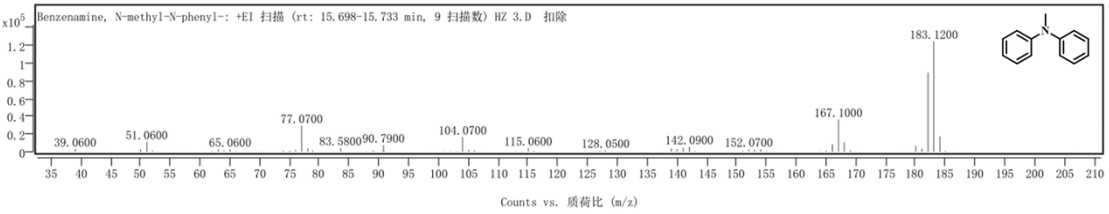

***N*-benzyl-3-bromoaniline**

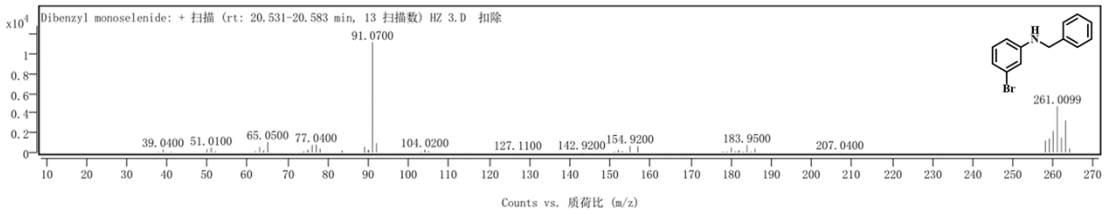

NMR spectra of selected products

N,N-Dimethylaniline

^{1}H NMR (600 MHz, Chloroform-*d*) δ 7.28 (d, *J* = 5.4 Hz, 2H), 6.78 (dd, *J* = 21.9, 7.8 Hz, 3H), 2.98 (s, 6H). ^{13}C NMR (151 MHz, Chloroform-*d*) δ 129.09, 112.79, 40.71.

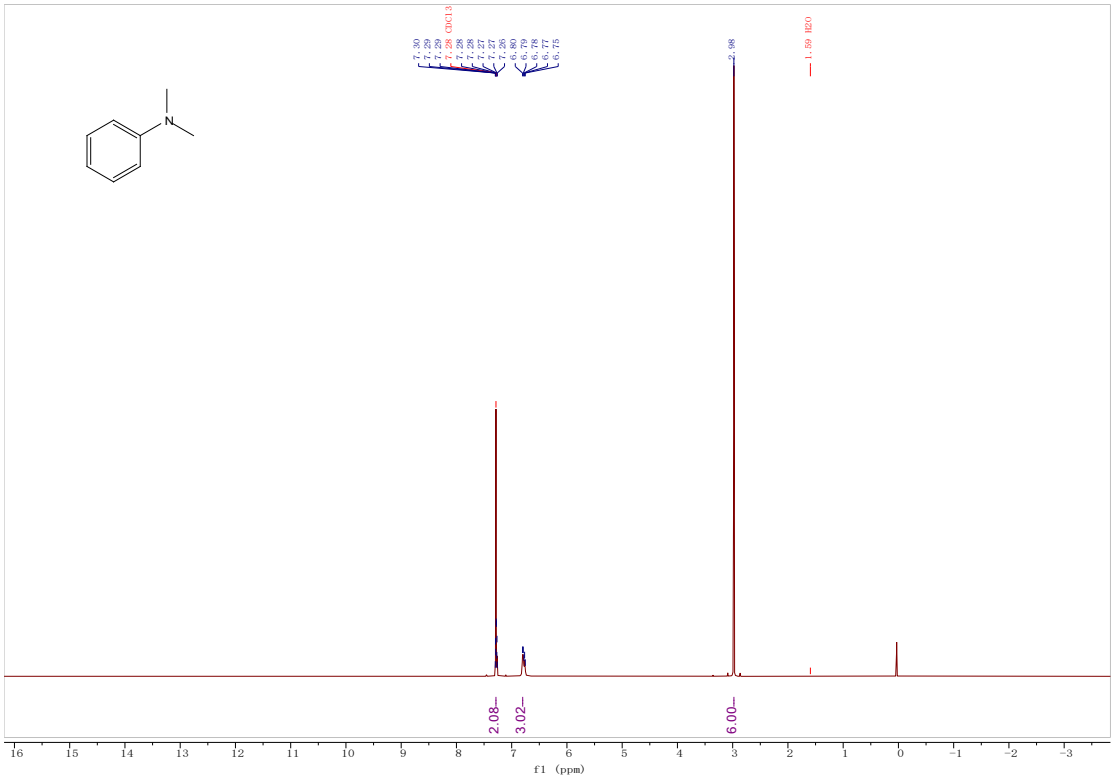

^{1}H NMR spectra of N,N-Dimethylaniline

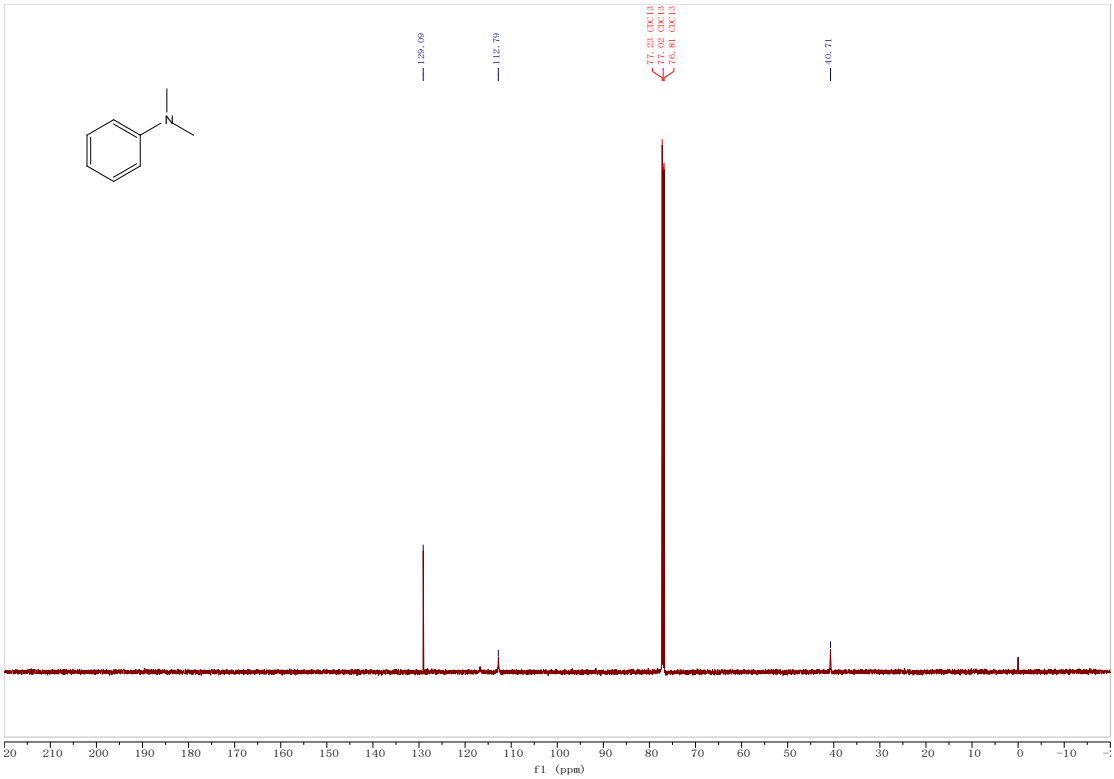

^{13}C NMR spectra of N,N-Dimethylaniline

***N*-Butylaniline**

^{1}H NMR (600 MHz, Chloroform-*d*) δ 7.26 – 7.14 (m, 2H), 6.82 – 6.51 (m, 3H), 3.15 (t, *J* = 7.1 Hz, 2H), 1.64 (p, *J* = 7.2 Hz, 2H), 1.47 (h, *J* = 7.4 Hz, 2H), 1.00 (t, *J* = 7.4 Hz, 3H). ^{13}C NMR (151 MHz, Chloroform-*d*) δ 148.47, 129.23, 117.19, 112.79, 43.77, 31.68, 20.32, 13.91.

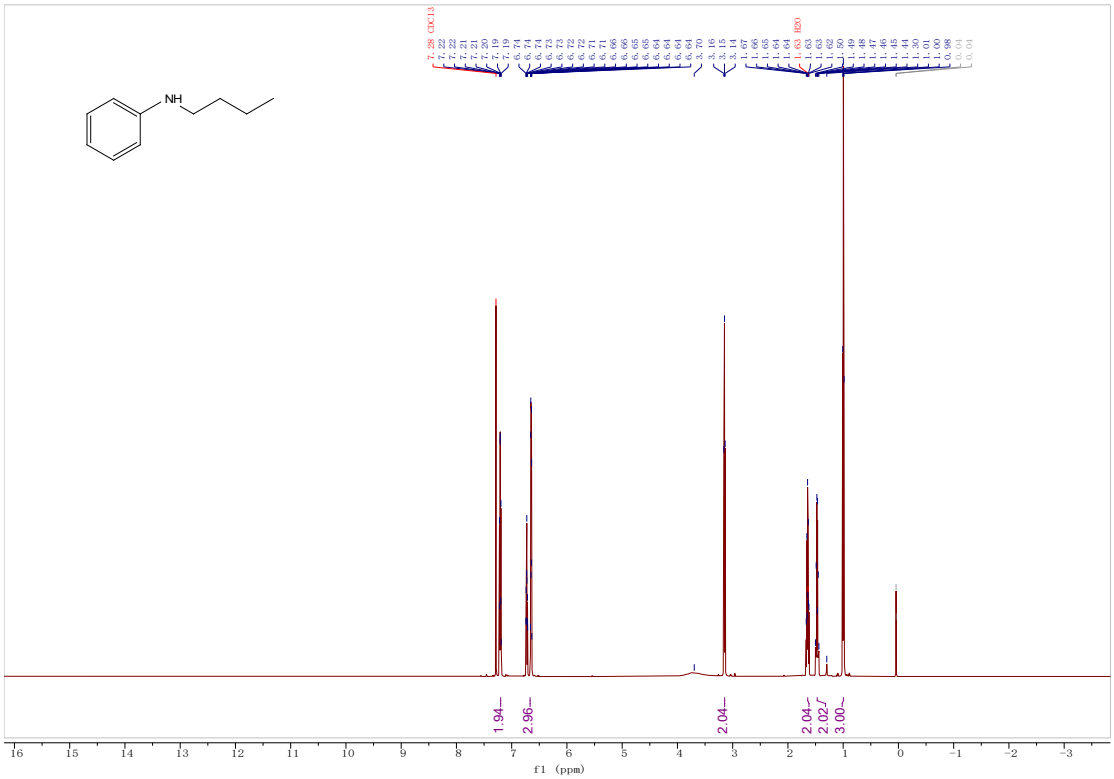

^{1}H NMR spectra of N-Butylaniline

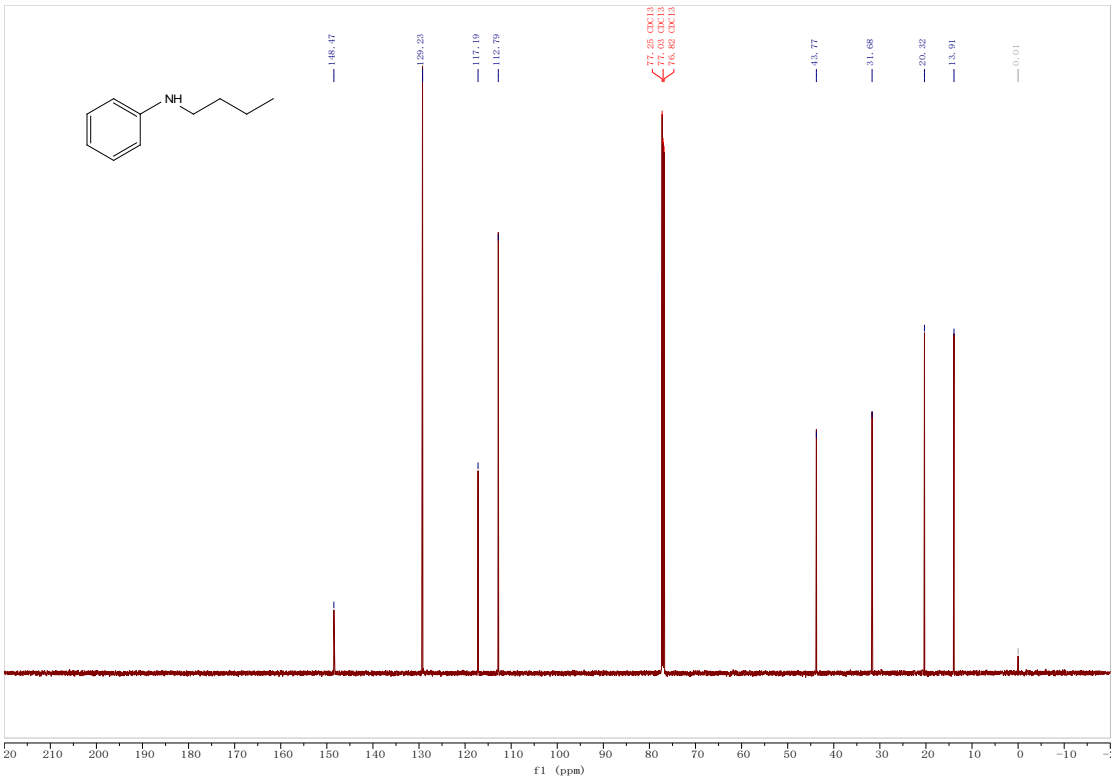

^{13}C NMR spectra of N-Butylaniline

***N*-Benzylaniline**

^{1}H NMR (600 MHz, Chloroform-*d*) δ 7.41 – 7.28 (m, 6H), 7.24 – 7.18 (m, 2H), 6.76 (dddd, *J* = 7.3, 6.2, 3.1, 1.8 Hz, 1H), 6.72 – 6.67 (m, 2H), 4.38 – 4.36 (m, 2H). ^{13}C NMR (151 MHz, Chloroform-*d*) δ 129.29, 128.65, 127.57, 127.27, 117.72, 112.99, 48.44.

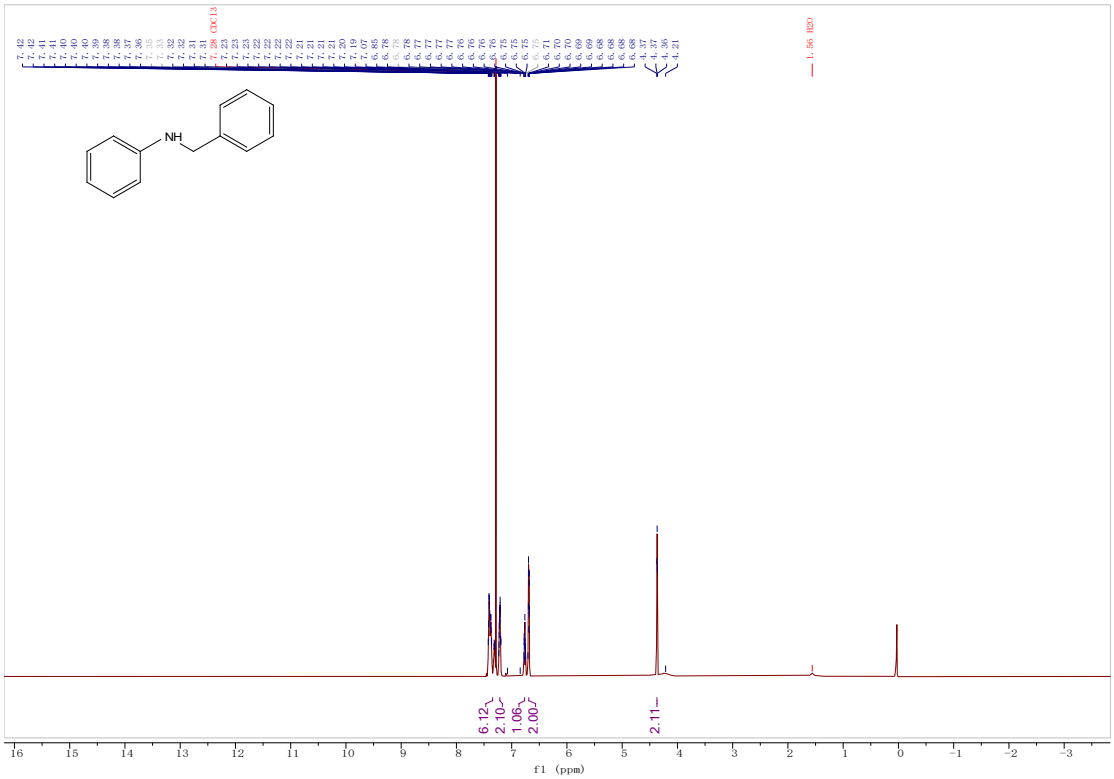

^{1}H NMR spectra of N-Benzylaniline

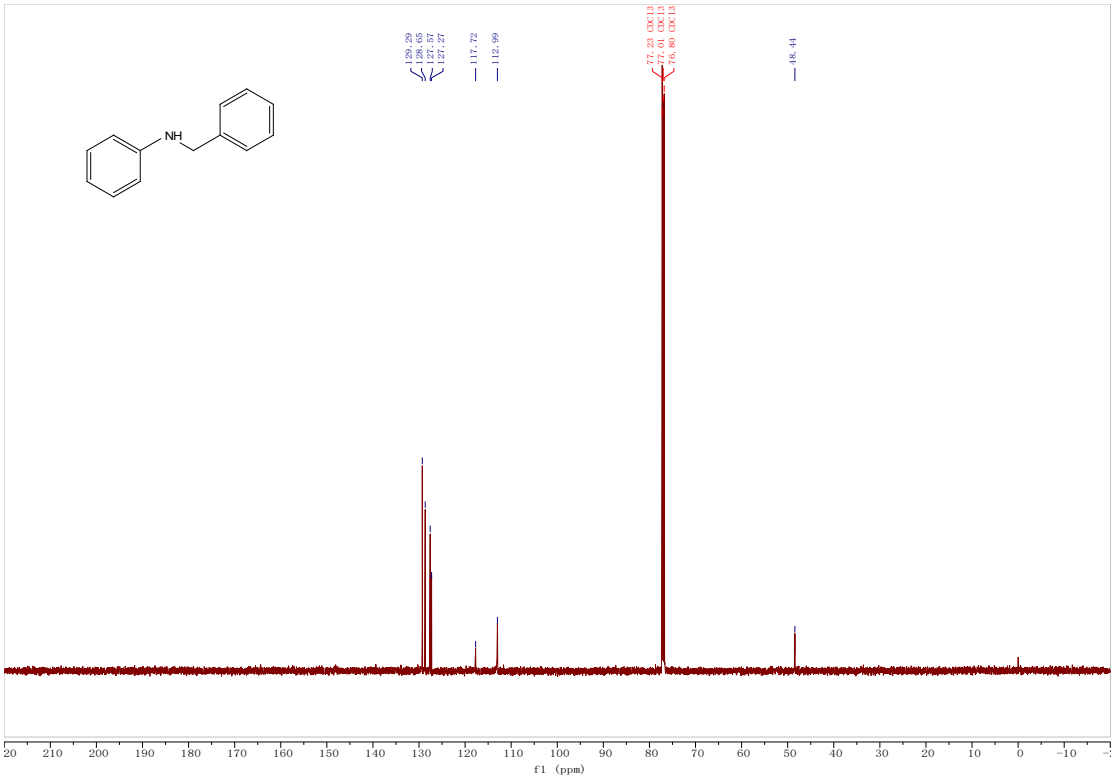

^{13}C NMR spectra of N-Benzylaniline

Dibenzylamine

^{1}H NMR (600 MHz, Chloroform-*d*) δ 7.40 – 7.27 (m, 10H), 3.85 (d, *J* = 1.2 Hz, 4H). ^{13}C NMR (151 MHz, Chloroform-*d*) δ 140.26, 140.22, 128.42, 128.19, 126.98, 53.15, 53.13.

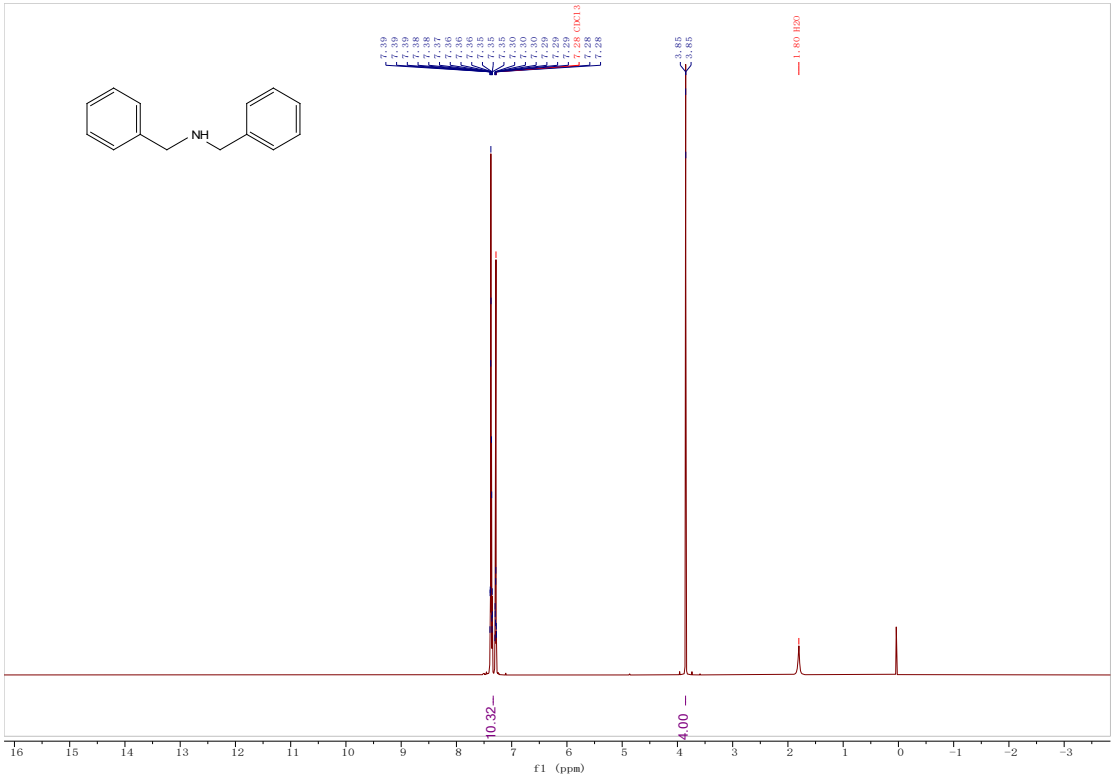

^{1}H NMR spectra of Dibenzylamine

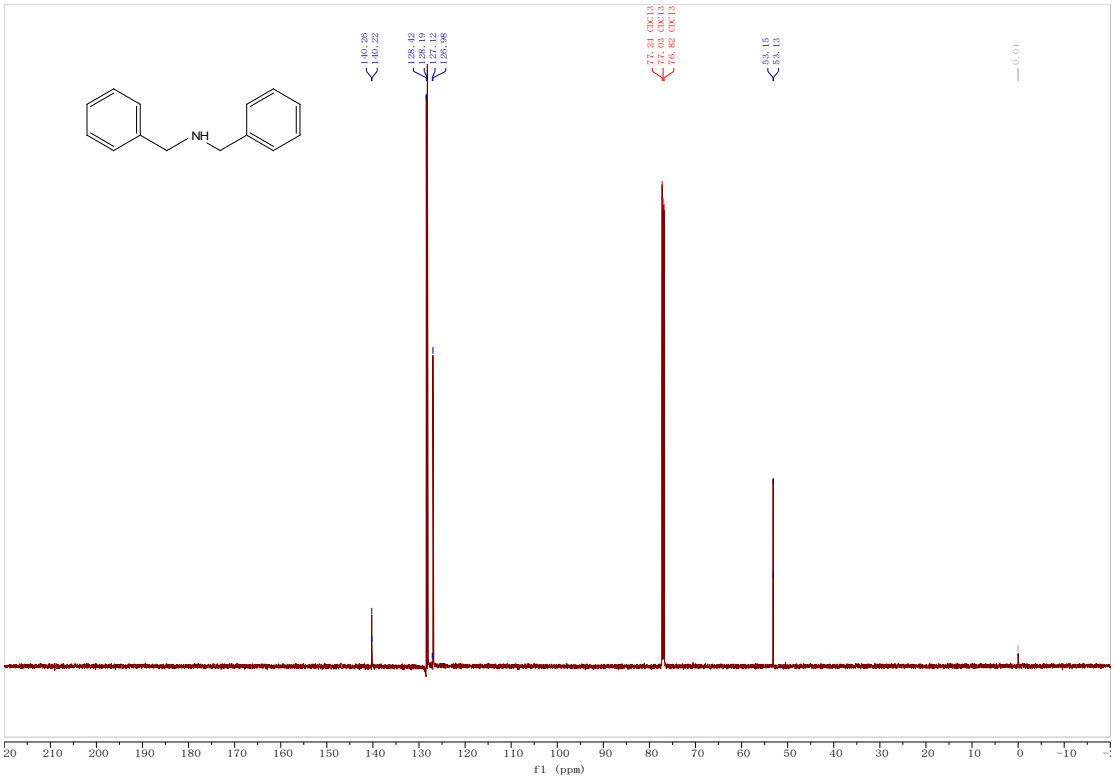

^{13}C NMR spectra of Dibenzylamine

***N,N*-Diethylaniline**

^{1}H NMR (600 MHz, Chloroform-*d*) δ 7.23 (t, *J* = 7.7 Hz, 2H), 6.77 – 6.55 (m, 3H), 3.38 (q, *J* = 7.0 Hz, 4H), 1.19 (t, *J* = 7.0 Hz, 6H). ^{13}C NMR (151 MHz, Chloroform-*d*) δ 147.85, 129.25, 115.37, 111.90, 44.32, 12.57.

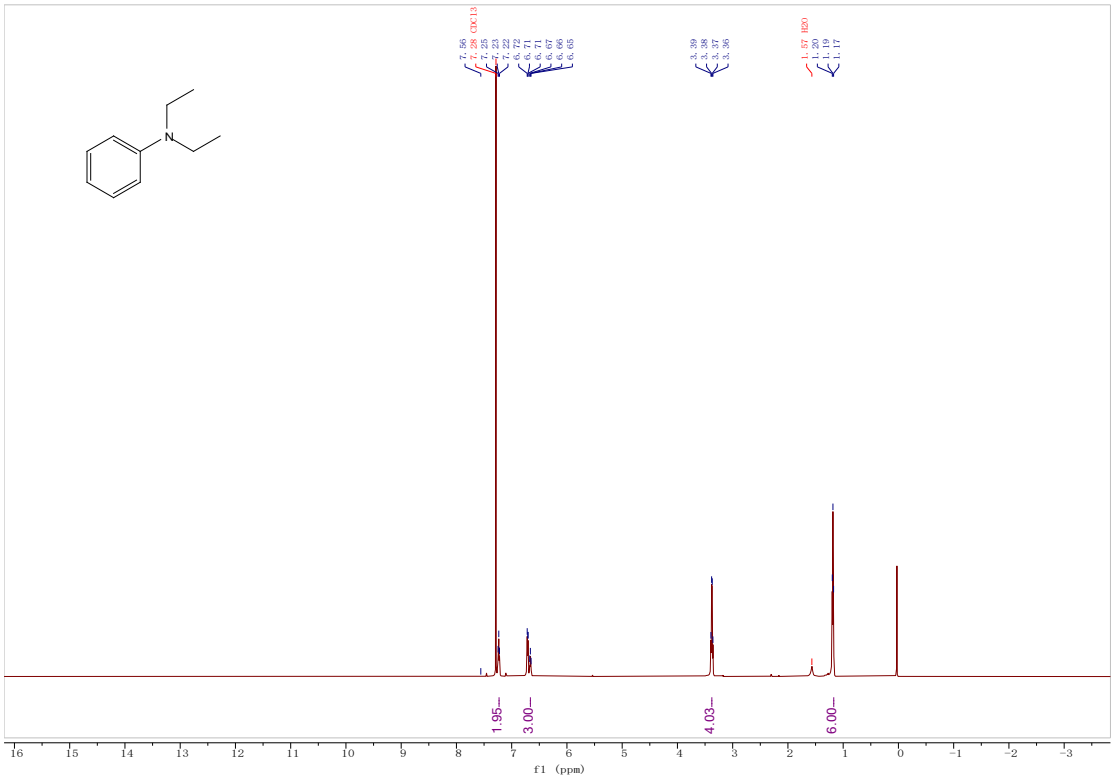

^{1}H NMR spectra of N,N-Diethylaniline

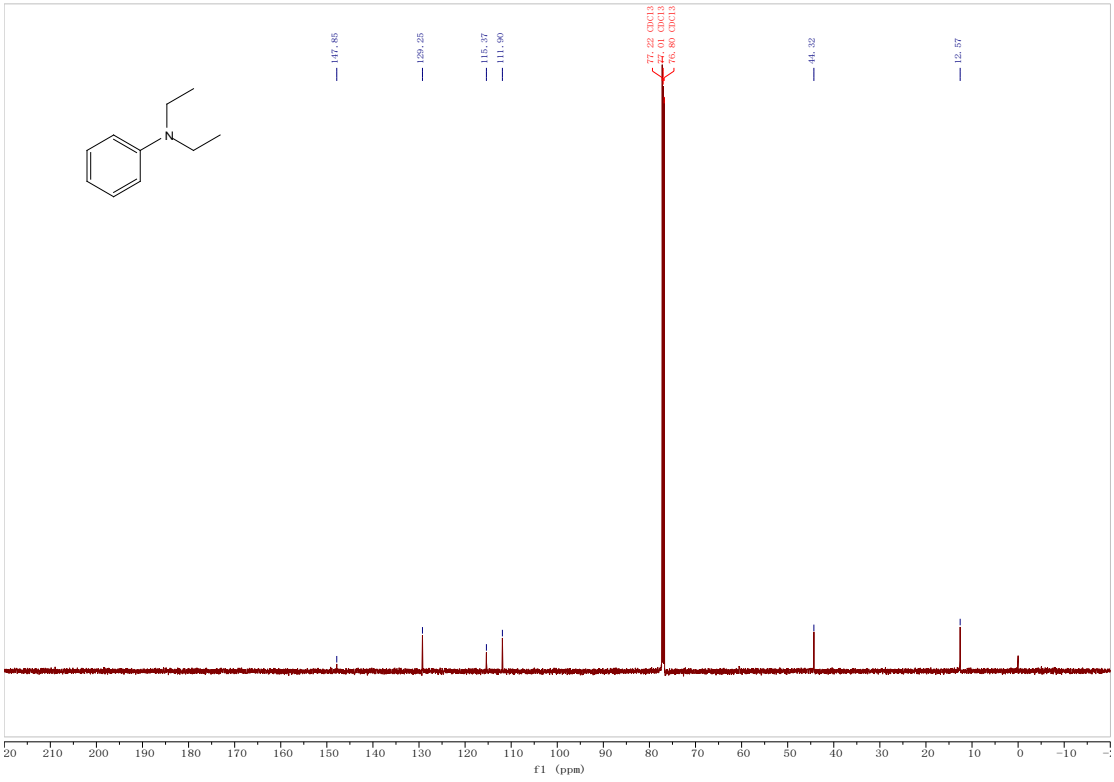

^{13}C NMR spectra of N,N-Diethylaniline

_N_-Benzyldiethylamine

^{1}H NMR (600 MHz, Chloroform-*d*) δ 7.42 – 7.30 (m, 4H), 7.28 – 7.24 (m, 1H), 3.62 (s, 2H), 2.66 – 2.50 (m, 4H), 1.09 (t, *J* = 6.6 Hz, 6H). ^{13}C NMR (151 MHz, Chloroform-*d*) δ 129.00, 128.16, 57.46, 46.70, 11.63.

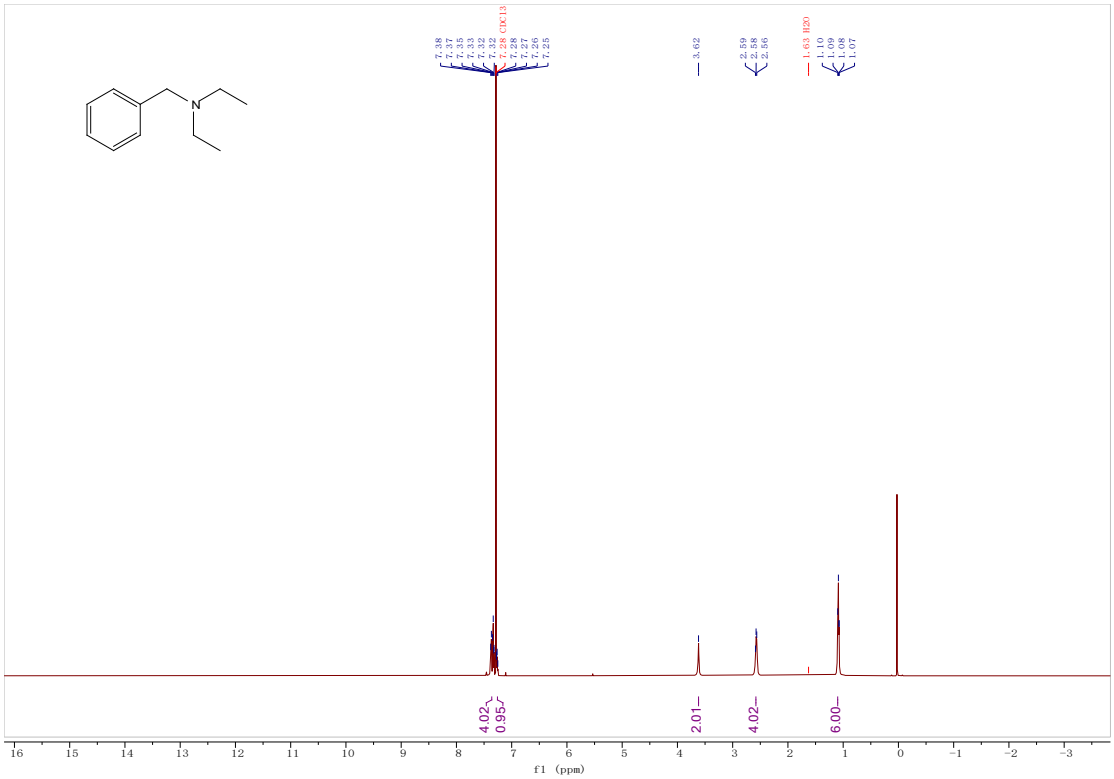

^{1}H NMR spectra of N-Benzyldiethylamine

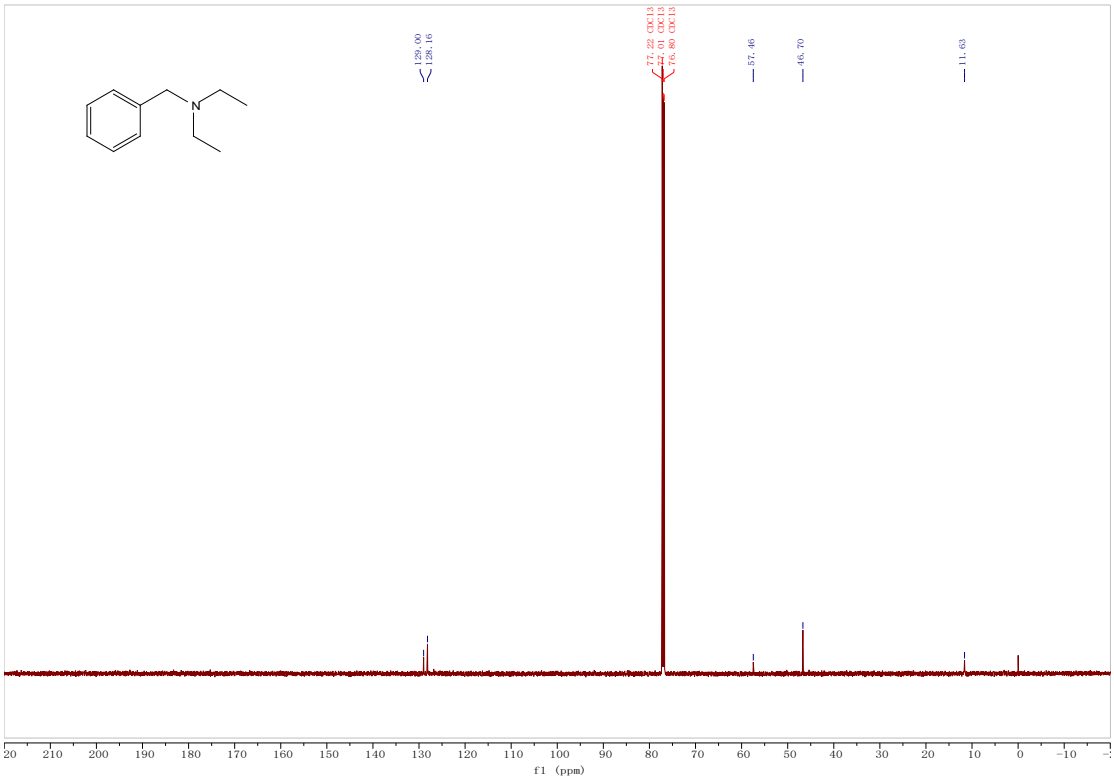

^{13}C NMR spectra of N-Benzyldiethylamine

_N_-benzyl-3-bromoaniline

^{1}H NMR (600 MHz, Chloroform-*d*) δ 7.43 – 7.30 (m, 5H), 7.04 (t, *J* = 8.0 Hz, 1H), 6.86 (dt, *J* = 7.8, 1.2

Hz, 1H), 6.82 (t, *J* = 2.1 Hz, 1H), 6.57 (dd, *J* = 8.2, 2.4 Hz, 1H), 4.33 (s, 2H). ^{13}C NMR (151 MHz, Chloroform-*d*) δ 149.19, 138.59, 130.52, 128.75, 127.56, 127.54, 127.51, 127.50, 123.29, 120.61, 120.53, 115.60, 111.70, 48.27, 48.22.

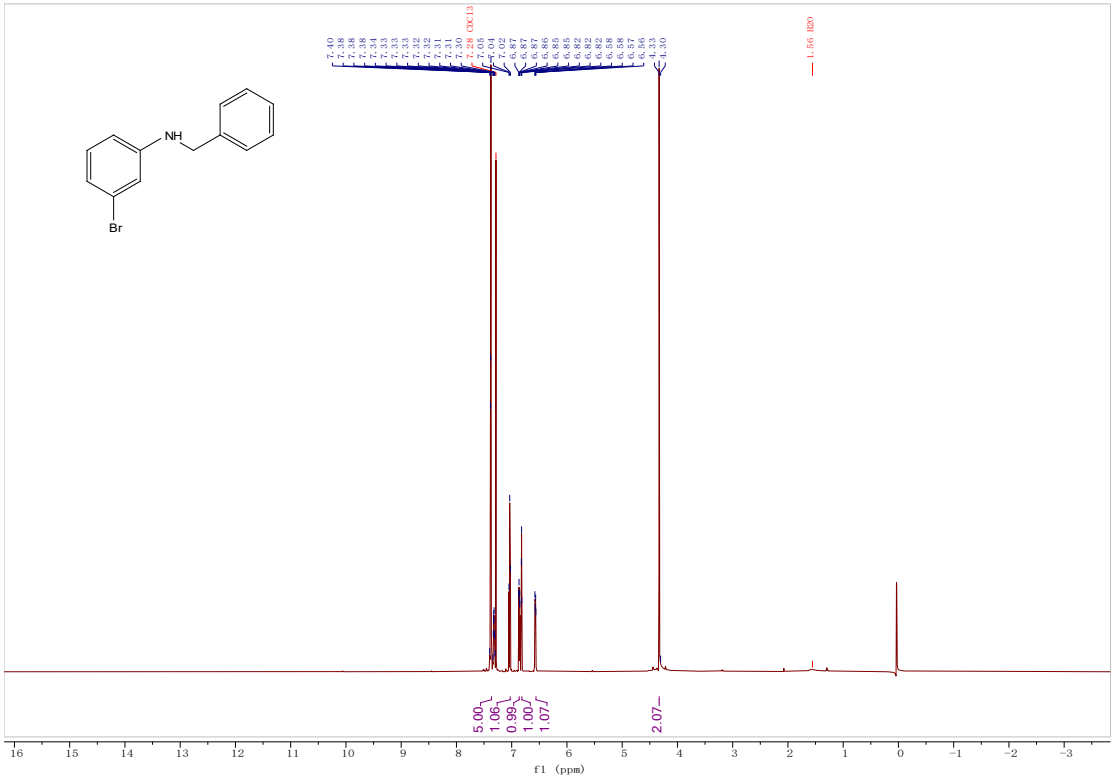

^{1}H NMR spectra of N-benzyl-3-bromoaniline

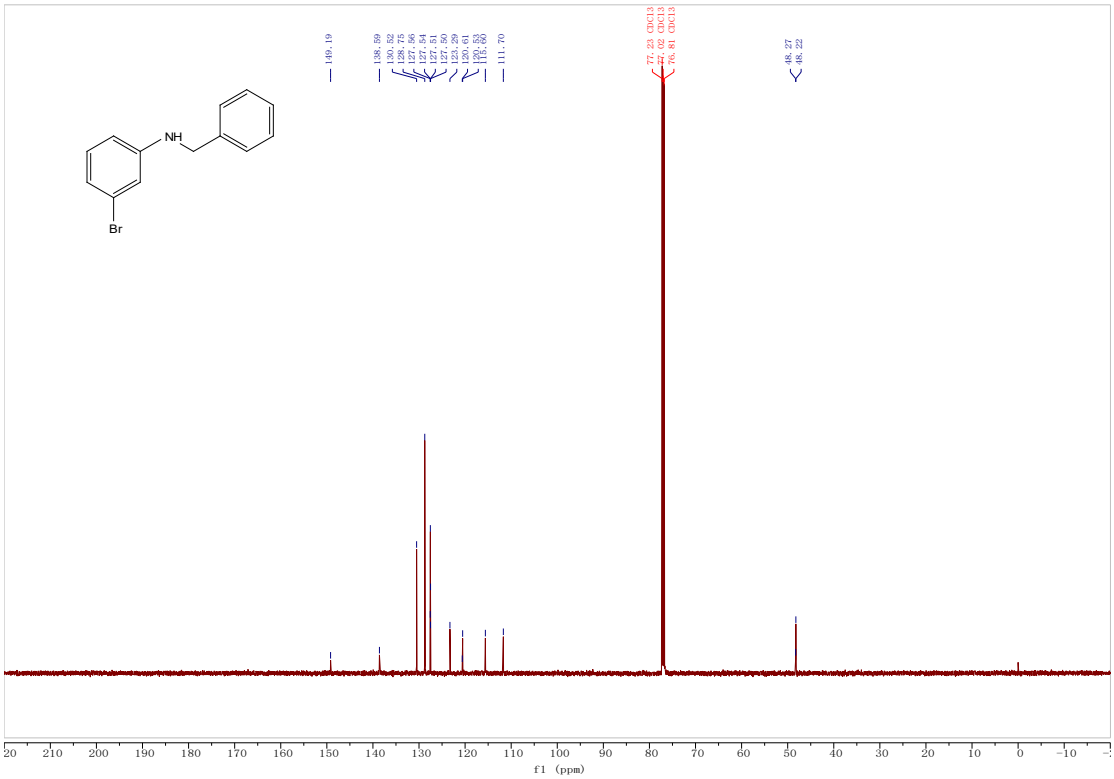

^{13}C NMR spectra of N-benzyl-3-bromoaniline

4-chloro-*N*,*N*-dimethylaniline

^{1}H NMR (600 MHz, Chloroform-*d*) δ 7.24 – 7.17 (m, 2H), 6.70 (t, *J* = 4.4 Hz, 2H), 2.96 (d, *J* = 1.4 Hz, 6H). ^{13}C NMR (151 MHz, Chloroform-*d*) δ 128.88, 40.84.

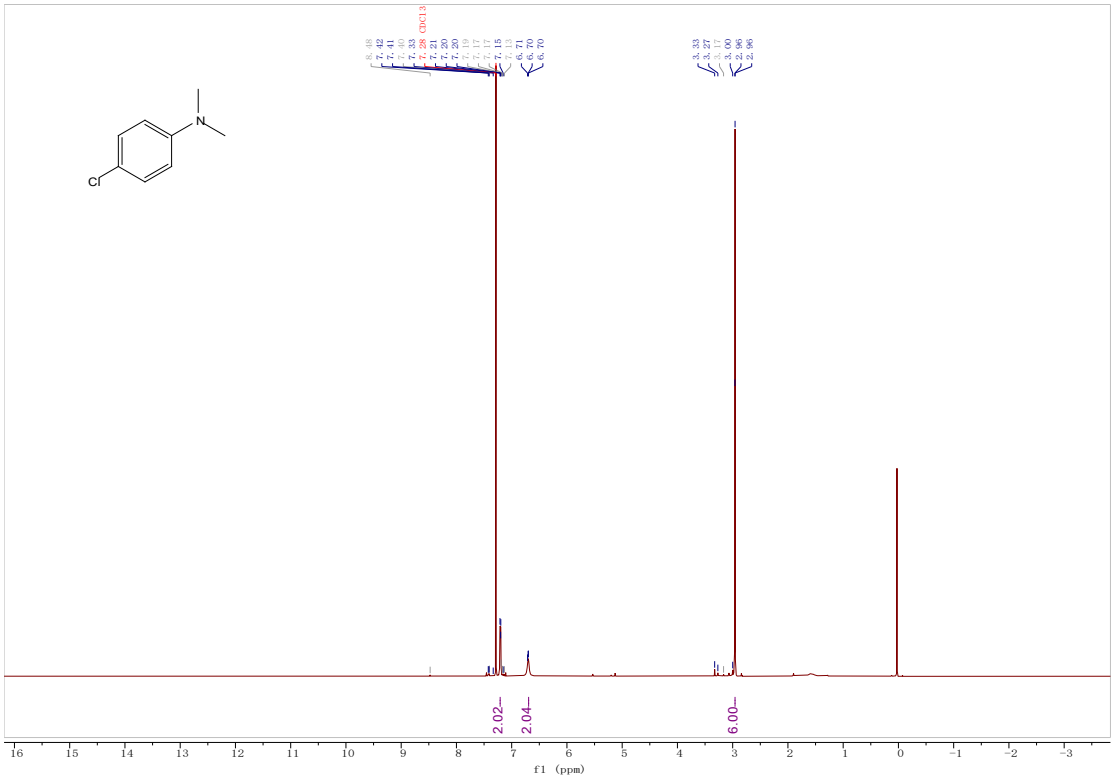

^{1}H NMR spectra of 4-chloro-N,N-dimethylaniline

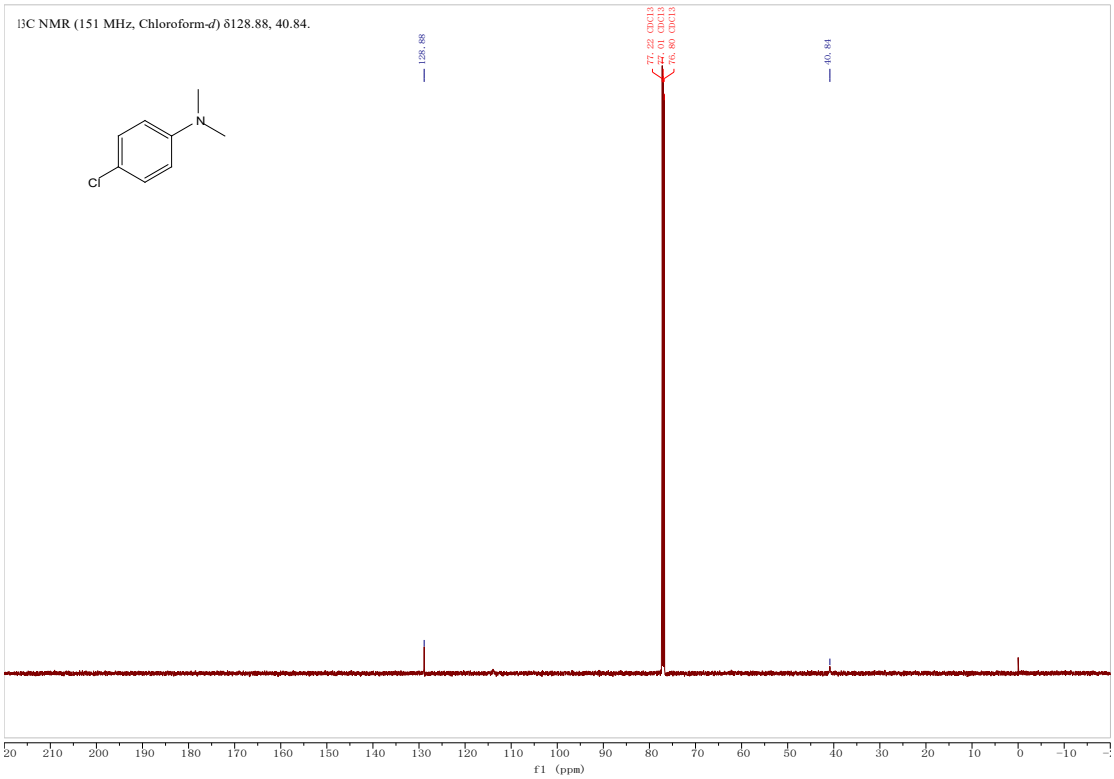

^{13}C NMR spectra of 4-chloro-N,N-dimethylaniline

Benzyldiisopropylamine

^{1}H NMR (600 MHz, Chloroform-*d*) δ 7.41 (d, *J* = 7.5 Hz, 2H), 7.31 (t, *J* = 7.5 Hz, 2H), 7.22 (t, *J* = 7.3 Hz, 1H), 3.67 (s, 2H), 3.06 (dd, *J* = 12.9, 6.7 Hz, 2H), 1.05 (d, *J* = 6.6 Hz, 12H). ^{13}C NMR (151 MHz, Chloroform-*d*) δ 143.29, 127.96, 127.89, 126.13, 48.91, 47.79, 20.76.

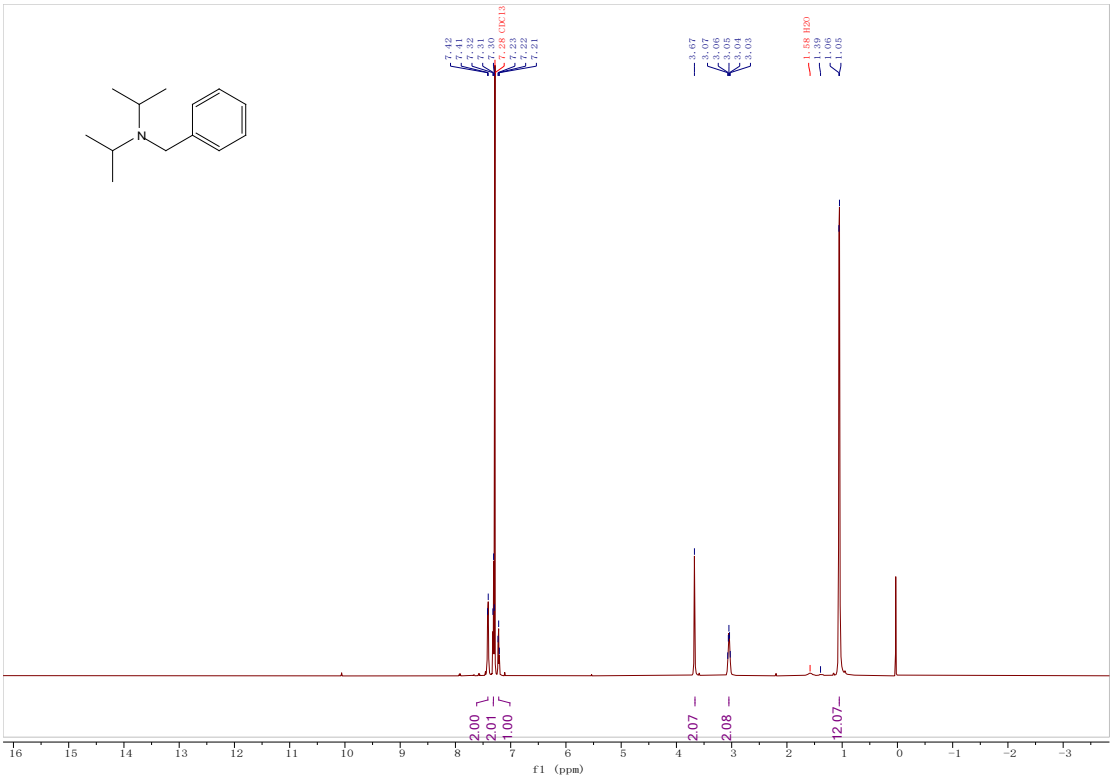

^{1}H NMR spectra of Benzyldiisopropylamine

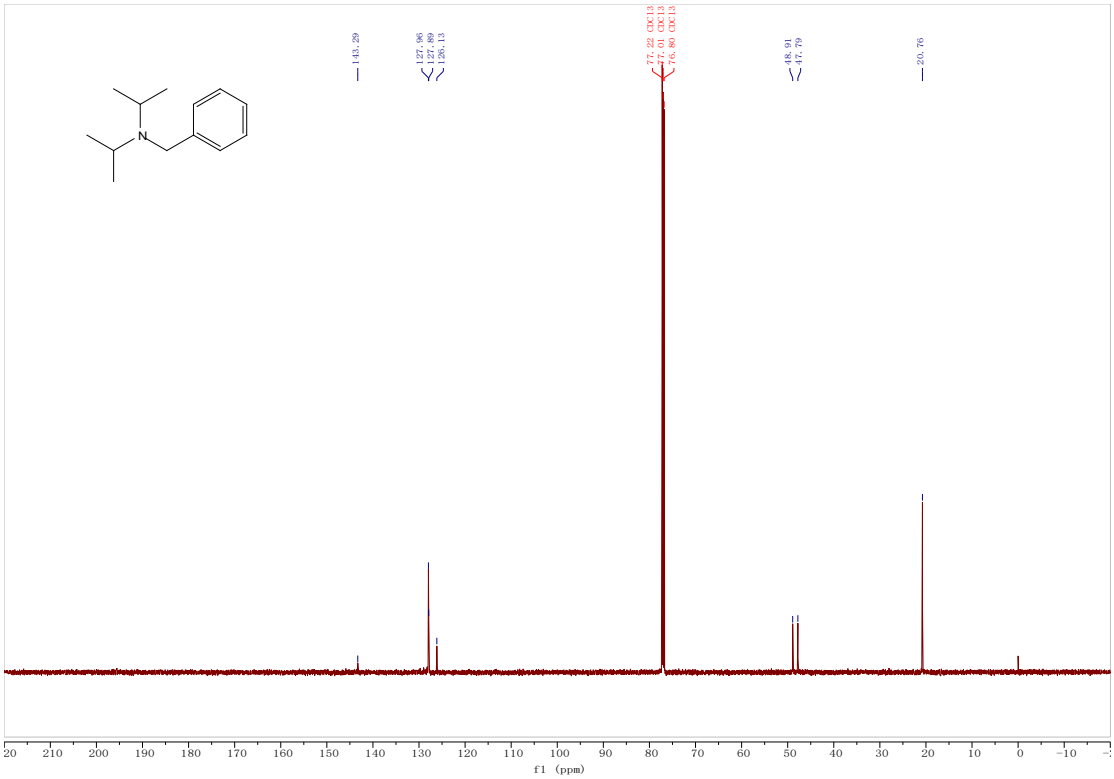

^{13}C NMR spectra of Benzyldiisopropylamine

_N_-Methyldiphenylamine

^{1}H NMR (600 MHz, Chloroform-*d*) δ 7.31 (dddt, *J* = 8.7, 7.5, 2.8, 1.6 Hz, 4H), 7.10 – 7.03 (m, 4H), 6.99 (dddd, *J* = 9.7, 7.2, 2.5, 1.3 Hz, 2H), 3.35 (dd, *J* = 2.8, 1.5 Hz, 3H). ^{13}C NMR (151 MHz, Chloroform-*d*) δ 149.03, 129.20, 121.33, 120.48, 40.28.

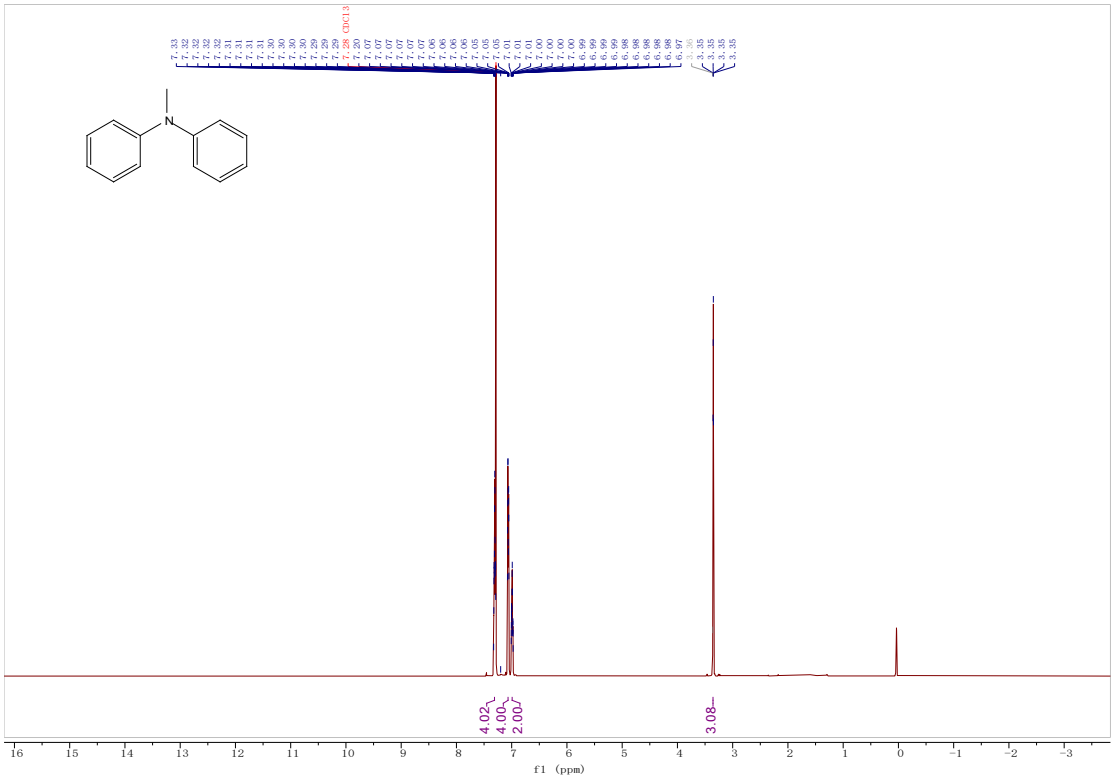

^{1}H NMR spectra of N-Methyldiphenylamine

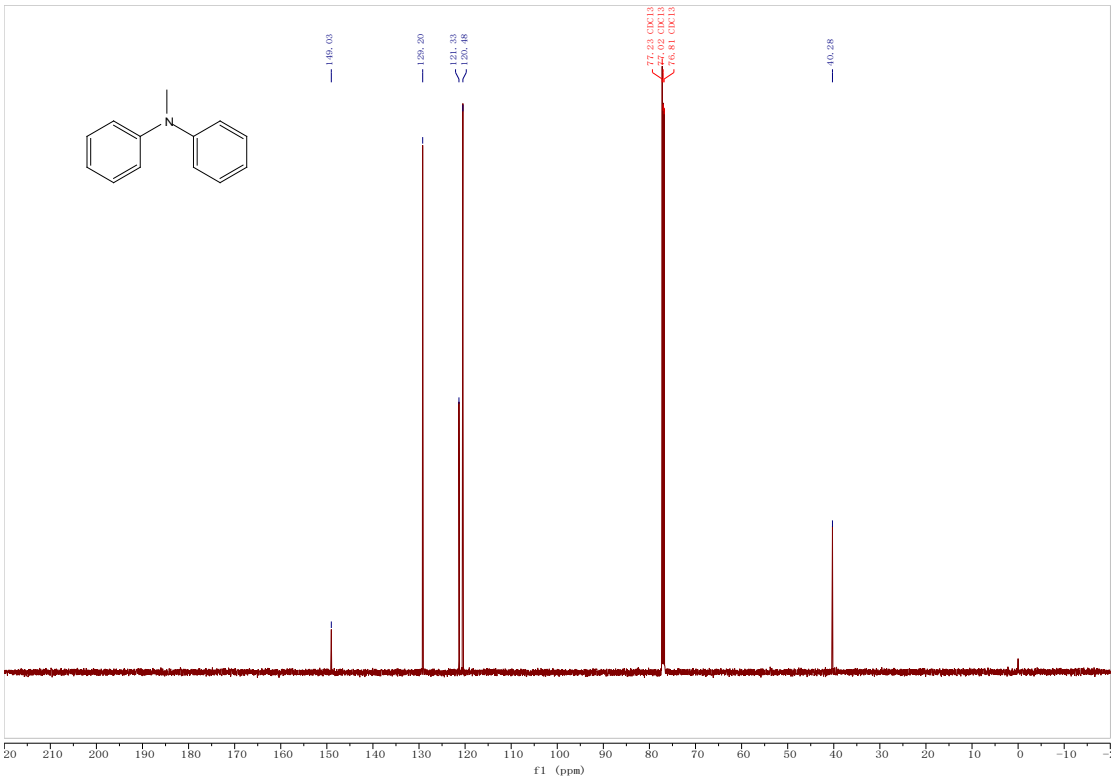

^{13}C NMR spectra of N-Methyldiphenylamine

_N_-Benzylpropanamine

^{1}H NMR (600 MHz, Chloroform-*d*) δ 7.35 (d, *J* = 4.4 Hz, 4H), 7.28 – 7.24 (m, 1H), 3.82 (s, 2H), 2.63 (t, *J* = 7.2 Hz, 2H), 1.55 (p, *J* = 7.3 Hz, 2H), 1.04 – 0.89 (m, 3H). ^{13}C NMR (151 MHz, Chloroform-*d*) δ 140.64, 128.37, 128.11, 126.85, 54.05, 51.39, 23.21, 11.78.

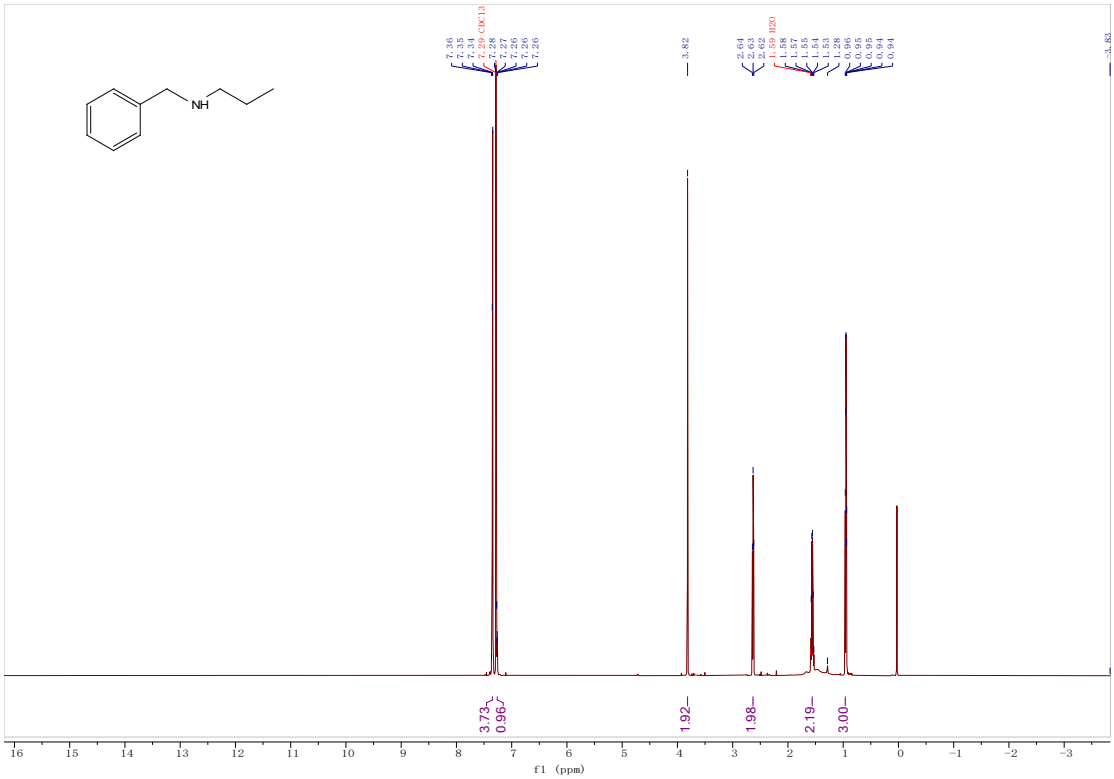

^{1}H NMR spectra of N-Benzylpropanamine

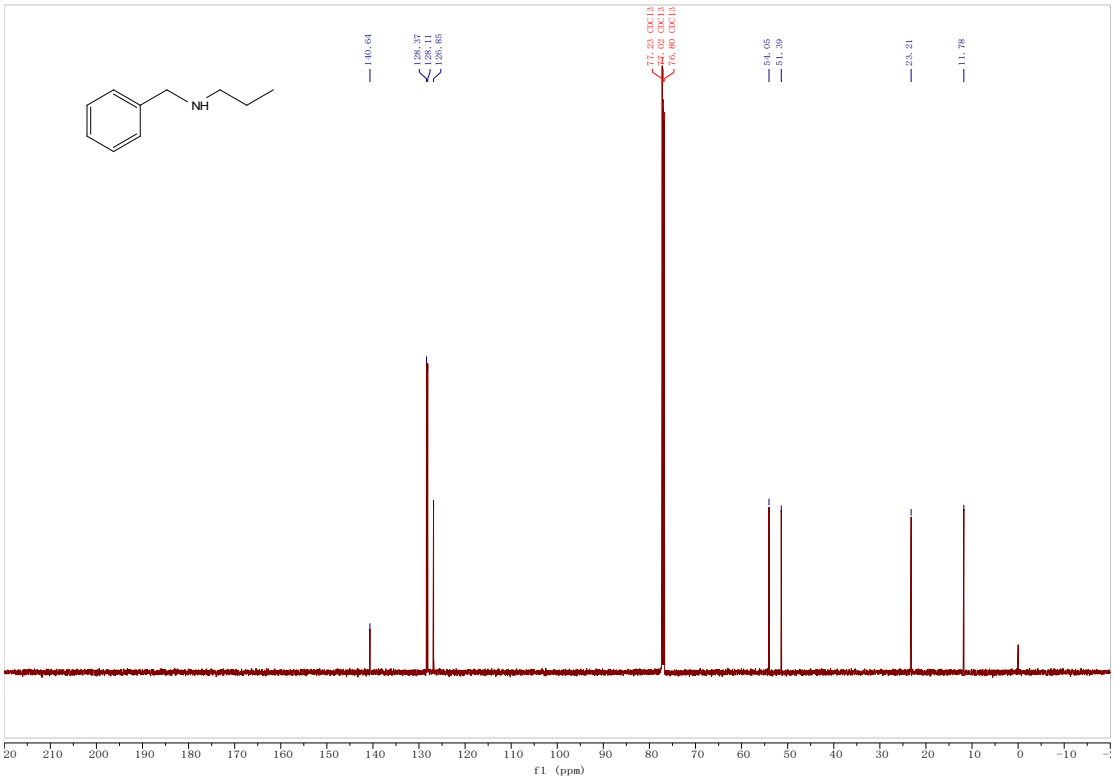

^{13}C NMR spectra of N-Benzylpropanamine

Computational Section

Figure S6. Stick model for Pd, Pd_1Pt_1 and Pt clusters

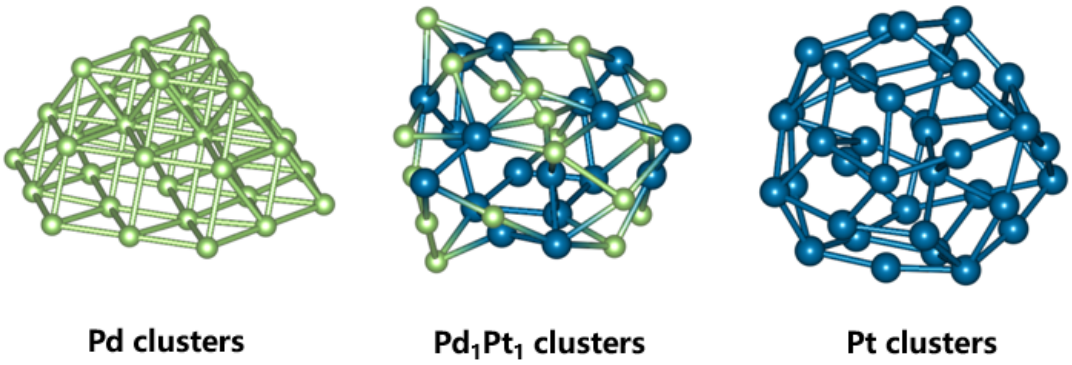

Computational Details

The structural optimization and the frequency analysis were performed at the GFN-xTB level of the xTB package.[2,3] Stationary points were optimized without symmetry constraint, and their nature was confirmed by vibrational frequency analysis.[4] To achieve this, a Gaussian interface to the xTB code "gau_xtb" was employed.[5] Analysis on the molecular orbitals was performed at the PBE0/def2-SV(P) level of theory using ORCA 4.2 package.[6]

References

1. Li, X.; Kang, B.; Dong, F.; Zhang, Z.; Luo, X.; Han, L.; Huang, J.; Feng, Z.; Chen, Z.; Xu, J.; Peng, B.; Wang, Z. L., Enhanced photocatalytic degradation and H_2/H_2O_2 production performance of S-pCN/$WO_{2.72}$ S-scheme heterojunction with appropriate surface oxygen vacancies. *Nano Energy* **2021,** *81*, 105671.
2. Bannwarth, C.; Ehlert, S.; Grimme, S., GFN2-xTB-An Accurate and Broadly Parametrized Self-Consistent Tight-Binding Quantum Chemical Method with Multipole Electrostatics and Density-Dependent Dispersion Contributions. *J. Chem. Theory Comput.* **2019,** *15* (3), 1652-1671.
3. Grimme, S.; Bannwarth, C.; Shushkov, P., A Robust and Accurate Tight-Binding Quantum Chemical Method for Structures, Vibrational Frequencies, and Noncovalent Interactions of Large Molecular Systems Parametrized for All spd-Block Elements (Z=1-86). *J. Chem. Theory Comput.* **2017,** *13* (5), 1989-2009.

4. Hratchian, H. P.; Schlegel, H. B., Using Hessian updating to increase the efficiency of a Hessian based predictor-corrector reaction path following method. *J. Chem. Theory Comput.* **2005,** *1* (1), 61-69.
5. Tian Lu, gau_xtb: A Gaussian interface for xtb code, http://sobereva.com/soft/gau_xtb.
6. Neese, F. Software Update: the ORCA Program System, Version 4.0. *WIREs Comput. Mol. Sci.* **2018,** 8, e1327.